Spitzer observations of acetylene bands in carbon-rich AGB stars in the Large Magellanic Cloud

M. Matsuura[1,2,3], P.R. Wood[4], G.C. Sloan[5], A.A. Zijlstra[1], J.Th. van Loon[6],
M.A.T. Groenewegen[7], J.A.D.L. Blommaert[7], M.-R.L. Cioni[8], M.W. Feast[9],
H.J. Habing[10], S. Hony[7], E. Lagadec[1], C. Loup[11], J.W. Menzies[12],
L.B.F.M. Waters[13,7], P.A. Whitelock[9,12,14]

[1] School of Physics and Astronomy, University of Manchester, Sackville Street, P.O. Box 88, Manchester M60 1QD, United Kingdom
[2] APS Division, Department of Pure and Applied Physics, Queen's University Belfast, University Road, BT7 1NN, United Kingdom
[3] National Astronomical Observatory of Japan, Osawa 2-21-1, Mitaka, Tokyo 181-8588, Japan
[4] Research School of Astronomy & Astrophysics, Mount Stromlo Observatory, Australian National University, Cotter Road,
Weston ACT 2611, Australia
[5] Astronomy Department, Cornell University, 610 Space Sciences Building, Ithaca, NY 14853-6801, USA
[6] Astrophysics Group, School of Physical and Geographical Sciences, Keele University, Staffordshire ST5 5BG, United Kingdom
[7] Instituut voor Sterrenkunde, KU Leuven, Celestijnenlaan 200B, 3001 Leuven, Belgium
[8] SUPA, School of Physics, University of Edinburgh, IfA, Blackford Hill, Edinburgh EH9 3HJ, United Kingdom
[9] Astronomy Department, University of Cape Town, 7701 Rondebosch, South Africa
[10] Sterrewacht Leiden, Niels Bohrweg 2, 2333 RA Leiden, The Netherlands
[11] Institut d'Astrophysique de Paris, CNRS, 98bis Boulevard Arago, 75014 Paris, France
[12] South African Astronomical Observatory, P.O.Box 9, 7935 Observatory, South Africa
[13] Astronomical Institute "Anton Pannekoek", University of Amsterdam, Kruislaan 403, 1098 SJ, Amsterdam,
The Netherlands
[14] NASSP, Department of Mathematics and Applied Mathematics, University of Cape Town, 7701 Rondebosch, South Africa

ABSTRACT

We investigate the molecular bands in carbon-rich AGB stars in the Large Magellanic Cloud (LMC), using the InfraRed Spectrograph (IRS) on board the *Spitzer Space Telescope* (SST) over the 5–38 μm range. All 26 low-resolution spectra show acetylene (C_2H_2) bands at 7 and 14 μm. The hydrogen cyanide (HCN) bands at these wavelengths are very weak or absent. This is consistent with low nitrogen abundances in the LMC. The observed 14 μm C_2H_2 band is reasonably reproduced by an excitation temperature of 500 K. There is no clear dilution of the 14 μm C_2H_2 band by circumstellar dust emission. This 14 μm band originates from molecular gas in the circumstellar envelope in these high mass-loss rate stars, in agreement with previous findings for Galactic stars. The C_2H_2 column density, derived from the 13.7 μm band, shows a gas mass-loss rate in the range 3×10^{-6} to $5 \times 10^{-5} M_\odot \, yr^{-1}$. This is comparable with the total mass-loss rate of these stars estimated from the spectral energy distribution. Additionally, we compare the line strengths of the 13.7 μm C_2H_2 band of our LMC sample with those of a Galactic sample. Despite the low metallicity of the LMC, there is no clear difference in the C_2H_2 abundance among LMC and Galactic stars. This reflects the effect of the 3rd dredge-up bringing self-produced carbon to the surface, leading to high C/O ratios at low metallicity.

Key words: stars: AGB and post-AGB – stars: atmospheres – stars: carbon – stars: mass-loss – Magellanic Clouds

1 INTRODUCTION

Low and intermediate mass stars (i.e. those with main sequences masses of 1–8 $M_\odot$) experience intensive mass loss towards the end of their life. During the asymptotic giant branch (AGB) phase, these stars lose up to 90% of their initial mass. As their population is large, AGB

stars are among the most important sources of gas and dust in the local universe.

Material lost from the star forms a circumstellar envelope, which consists of gas and dust grains. In this circumstellar envelope, various kinds of molecules exist. The molecules first form in the stellar photosphere. In the circumstellar envelope, an active chemistry, particularly in regions where interstellar UV radiation penetrates, leads to further molecules (Millar et al. 2000). However, the structure of the circumstellar envelope and the formation region of these molecules are not yet completely understood. Molecules are also formed in the innermost regions of the envelope where the stellar pulsations set up shock waves (Durai and Hatchell 2000; Gautschy-Loidl et al. 2004). Around carbon-rich stars, which have a carbon to oxygen ratio of C/O>1, CO, HCN and C_2H_2 and many carbon chain molecules are detected. C_2H_2, which is the focus of this paper, is one of the most abundant molecules after CO in carbon-rich envelopes. Note in particular that C_2H_2 may be important for dust formation in carbon stars (Keady & Hinkle 1988).

The majority of nearby galaxies have a lower metallicity than the Milky Way. The metallicity of red giants in the Galactic disk ranges from [Fe/H]=−0.11 to +0.06 (Smith & Lambert 1985). The mean metallicity of the Large Magellanic Cloud (LMC) is about half of the solar metallicity. The metallicity for LMC AGB stars is uncertain, but may be similar to that found in red giants from [Fe/H]=−1.1 to [Fe/H]=−0.3 (Smith et al. 2002). A lower metallicity should affect the abundances of molecules in cool stars. However, for AGB stars, carbon atoms are synthesised in the core and brought to the surface by the third dredge-up. Therefore, abundances of carbon-bearing molecules depend on the balance of the low metallicity effect and the enrichment of carbon atoms through nuclear synthesis. Previous studies (Matsuura et al. 2002b, 2005) using 3-μm spectra have found that the C_2H_2 abundance is higher in carbon-rich stars in the LMC than in similar stars our Galaxy. This was first suggested by a study of the 3.1 μm HCN+C_2H_2 band (van Loon et al. 1999). However, 3-μm C_2H_2 is a mixture of photospheric origin and circumstellar origin (van Loon et al. 2006), and the influence of the temperature of the central star is not negligible. In this study, we use *Spitzer* mid-infrared spectra covering the 13.7 μm C_2H_2 bands. These bands are predominantly of circumstellar origin and, therefore, we are able to study the molecular abundance in the circumstellar envelope, including the gas mass-loss rate and metallicity effects. The *Spitzer Space Telescope* enables us to carry out a study of the 13.7 μm C_2H_2 band in AGB stars in the LMC, for the first time.

2   OBSERVATIONS AND ANALYSIS

Spectra of carbon stars in the LMC have been obtained using the InfraRed Spectrograph (Houck et al. 2004, IRS) on board the *Spitzer Space Telescope* (SST). The stars were observed as part of the General Observing time of SST, programme 3505 (P.I. P.R. Wood).

Two low-resolution modules Short-Low (SL) and Long-Low (LL) were used, which provide wavelength coverage from 5–38 μm and spectral resolution from R=70–130. Spectra were covered by four segments, namely SL 2nd order (5.3–8.7 μm), SL 1st order (7.4–14.5 μm), LL 2nd order (14.0–21.3 μm) and LL 1st order (19.5–38.0 μm). In addition, extra-spectra were obtained with 'bonus' segments (7.3–8.8 and 20–22 μm). The 7-μm C_2H_2 bands fall on two segments, which could leave some uncertainty in the overlap region. (Zijlstra et al. 2006) provide an overview of the project and describe the details of target selection, observations and data-reduction.

For the analysis, we calculate synthetic spectra of HCN and C_2H_2 molecular bands using the line lists from the HITRAN database, 2004 edition (Jacquemart et al. 2003; Rothman et al. 2005). The partition function of C_2H_2 is available up to a temperature of 500 K, therefore, the modelling is limited to this temperature range. There are insufficient lines in the model at 7 μm and this band cannot therefore be reproduced. Calculation codes are described in Matsuura et al. (2002a); a slab local thermodynamic equilibrium (LTE) model with a single excitation temperature and a single column density is used. The model is intended to identify the molecular bands and to estimate their approximate excitation temperatures and density. Thus, this procedure does not reveal fully the atmospheric structure of the AGB stars. One of the uncertainties is any effect due to spherically symmetric structure. In the slab model, molecular emission from the circumstellar envelope is not considered, thus, the column densities tend to be higher solved for this slab model than they would be for spherical symmetric structure.
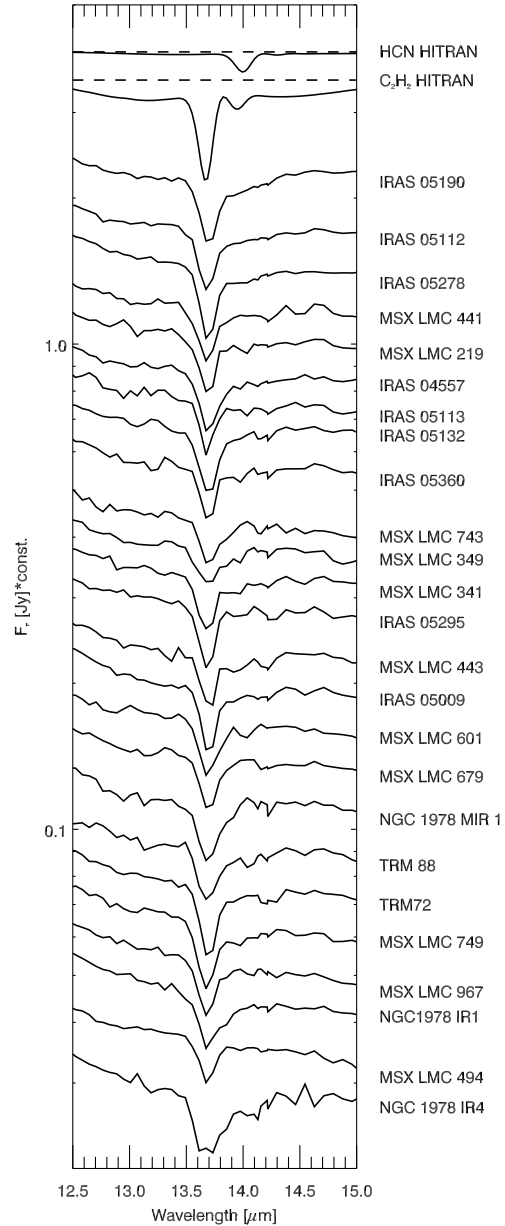
3   DESCRIPTION OF SPECTRA

Fig. 1 shows the 7 μm region of the Spitzer spectra, arranged in order of the infrared colour [6.4]−[9.3]. From bottom to top, the colour becomes redder (hereafter, 'redder' means that the ratio of long-wavelength to short-wavelength flux is larger). The definition of the colour (the 'Manchester system') can be found in Zijlstra et al. (2006) and Sloan et al. (2006). A double-peaked molecular absorption band centred at 7.5 μm is found in all of the spectra. This absorption is associated with the C_2H_2 $\nu_4^1 + \nu_5^1$ bands (P- and R-branches), which are found in the model spectrum of C_2H_2. A synthetic spectrum of C_2H_2 is plotted at the top of Fig. 1. (The model uses an excitation temperature of T_{ex} =500 K, and a column density of $n = 1 \times 10^{20}$ cm^{-2}.) There are insufficient C_2H_2 lines included in HITRAN to reproduce the shape (depth and width) of this feature. Nevertheless, the synthetic spectrum confirms the identification of this feature from the wavelength. Because of the incompleteness of the line list at this wavelength range, the column density derived from the 7 μm feature is not reliable.

Around 7 μm, other molecular bands have been found in Galactic carbon stars. Aoki et al. (1998) re-
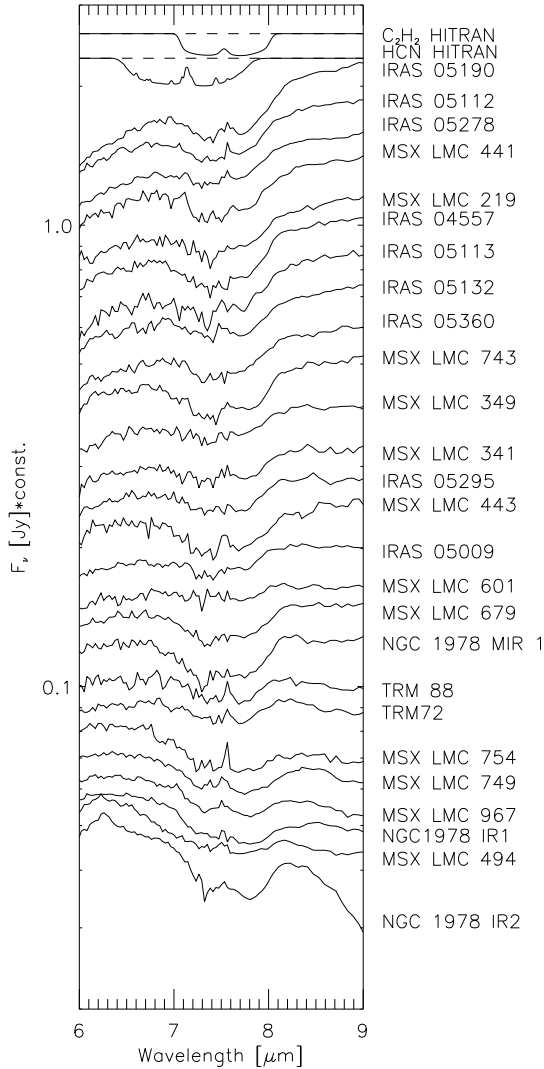
Figure 1. Spitzer spectra around 7.5 μm of LMC carbon stars, showing the C_2H_2 band. The spectra are sorted in order of the decreasing [6.4]−[9.3] infrared colour from top to bottom. Model spectra of C_2H_2 and HCN are used to identify the molecular bands (C_2H_2 absorption is amplified in intensity by a factor of 2.5).

Figure 2. Acetylene band at 13.7 μm from the Spitzer spectra, in the same order as Fig. 1.

ported a SiS first overtone band at 6.6–7 μm. This band is relatively weak (less than 5 % absorption with respect to the continuum, except for a few contributing lines) according to Aoki et al. (1998), and such a weak band cannot be clearly detected in our LMC spectra. The HCN $2\nu_2{}^0$ P-branch and R-branch are found at about 6.5–7.7 μm (Carter et al. 1993; Rothman et al. 2005). Fig. 1 also includes the HCN model profile. This molecule may be responsible for the shallow suspected absorption in NGC 1978 IR4 and MSX LMC 494. Except for these cases, the presence of HCN bands is not clear at low wavelength resolution. CS fundamental bands are found at 7–8 μm with a bandhead at 7.3 μm (Aoki et al. 1998). This feature is not detected in the spectra discussed here. This is probably because CS is masked by strong C_2H_2 bands, while the Aoki et al.

(1998) sample consists of relatively warm carbon stars and C_2H_2 molecules are not formed efficiently in the hotter photospheres (Tsuji 1981).

Fig. 2 shows the 14 μm region of the Spitzer spectra sorted in the same order as in Fig. 1. A sharp absorption band at 13.7 μm is found in all of the spectra. This feature is due to the Q-branch band of the C_2H_2 fundamental ν_5 and other transitions involving ν_5. The P- and R-branches of C_2H_2 produce broad absorption features in the synthetic spectrum on either side of the Q-branch band. There is a second peak of C_2H_2 absorption at 13.9 μm, and this band may also be found in the observed spectra. As a reference, we show the model

Table 1. Model parameters

Name	Molecule	Column density
IRAS 05278−6942	C_2H_2	1×10^{18}
IRAS 05112−6755	C_2H_2	4×10^{17}
MSX LMC 494	C_2H_2	4×10^{17}
MSX LMC 601	C_2H_2	9×10^{17}
	HCN	1×10^{17}
TRM 88	C_2H_2	9×10^{17}

spectra of C_2H_2 ($n = 1 \times 10^{18}\,\mathrm{cm}^{-2}$, $T_\mathrm{ex} = 500\,\mathrm{K}$) and HCN ($n = 3 \times 10^{17}\,\mathrm{cm}^{-2}$, $T_\mathrm{ex} = 500\,\mathrm{K}$).

Cernicharo et al. (1999) and Aoki et al. (1999) studied ISO spectra of Galactic carbon stars: they found that two molecular bands are blended in the 13–14 μm range, namely $C_2H_2\,\nu_5$ (and other transitions involving ν_5) and HCN fundamental ν_2^{1}. Fig. 3 shows some example ISO/SWS spectra. Hony et al. (2002) initially presented these ISO/SWS data, illustrating AGB stars and planetary nebulae. The ISO/SWS AOT1 resolution of $R \sim 300$ is higher than that of the Spitzer/IRS. The characteristic absorption features of these two molecules are clearly separated. The C_2H_2 band is centred at 13.7 μm, while the sharp absorption of HCN is found at 14 μm. In addition, the HCN bands are occasionally found in emission (Aoki et al. 1999; Cernicharo et al. 1999), as seen in IRC+50 096 and AFGL 2310 (Fig. 3).

From the ISO/SWS spectra, we define representative spectra, which show (1) C_2H_2 only (2) C_2H_2+ HCN in absorption (3) C_2H_2+ HCN in emission. Within category (1), there are two sub-categories, which contain hot C_2H_2 traced by a prominent 13.9 μm feature (Aoki et al. 1999), and cold C_2H_2 without that feature.

Among our LMC spectra, there is a possible detection of 14.0 μm HCN absorption in TRM 88 and MSX LMC 601. Apart from these sources, there is no clear detection of HCN either in emission or in absorption. In addition, the 13.9 μm C_2H_2 absorption is also weak; there is no LMC spectrum with C_2H_2 comparable to the Galactic carbon star S Sct, which shows a strong secondary C_2H_2 absorption feature at 13.9 μm in addition to the broad feature at 13.7 μm C_2H_2. This shows that C_2H_2 in our LMC sample is relatively cold.

In Fig. 4, we fit representative LMC spectra with the model. The column density of C_2H_2 is 4×10^{17}–1×10^{18} cm^{-2} (Table 1). A model spectrum of HCN is also added to C_2H_2 spectrum for a comparison with MSX LMC 601 spectrum. The column density of HCN is 1×10^{17} cm^{-2}.

4   NON-DILUTION

The spectra in Fig. 2 are sorted in order of colour, [6.4]−[9.3], so that the colour increases from bottom to top. Note particularly that the 13.7 μm Q-branch band does not fade away towards redder stars. The [6.4]-[9.3] colour increases mainly as the contribution of the dust emission increases relative to the stellar emission. The [6.4]−[9.3] colour is a measure of the optical depth of the shell, and therefore of the mass-loss rate; the 13.7 μm
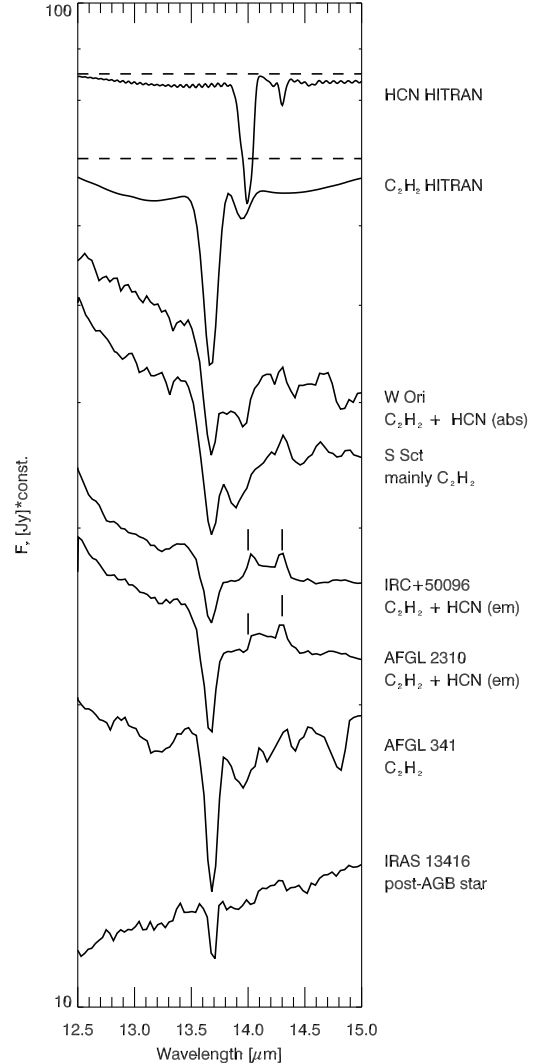
Figure 3. Representative spectra of the C_2H_2 and the HCN bands found in the ISO spectra of Galactic carbon stars.

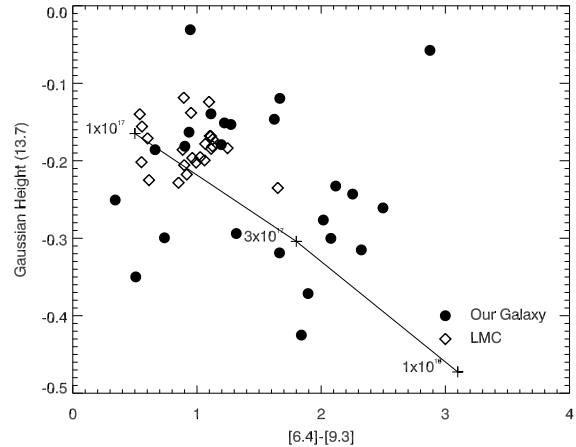C_2H_2 does not weaken towards more highly obscured stars, i.e., higher mass-loss rate stars.

This result is in contrast to other C_2H_2 bands, such as the 3.1 μm HCN+C_2H_2 band and the 3.8 μm C_2H_2 band (e.g. van Loon et al. 1999, 2006; Matsuura et al. 2002b, 2005) where the 3-μm band equivalent width is observed to be smaller in redder carbon stars. This difference between the 13-μm and 3-μm bands cannot be a consequence of differences between the stars examined. Both this work and Matsuura et al. (2005) discuss stars with similar near-infrared colours ($1 < H - K < 3$, and $0.3 < H - K < 3.2$ respectively). IRAS 05112−7655 was indeed observed here and in van Loon et al. (1999) and Matsuura et al. (2005). Therefore, the 13.7 μm C_2H_2 band behaves in a different way with mass-loss rate from the bands at shorter wavelength. The decreasing equivalent width of the 3.8 μm bands can be explained if dust emission fills in the absorption band. There is no obvious evidence of such dilution by dust within the
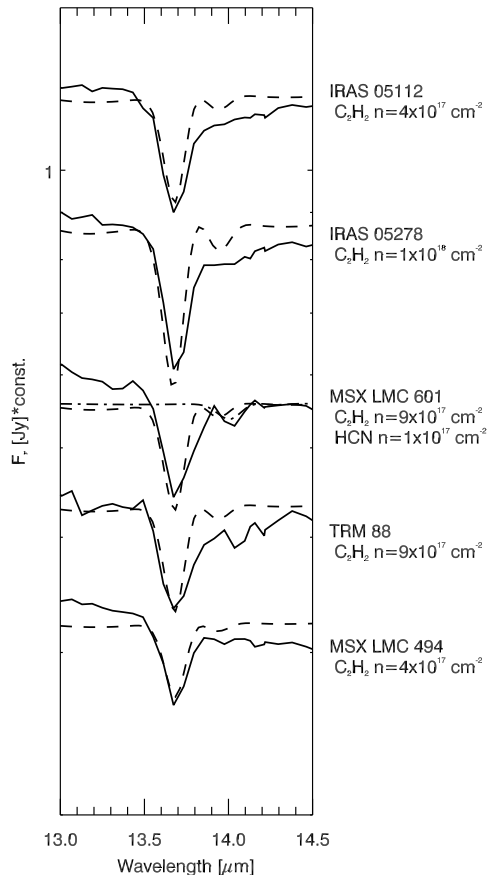
Figure 4. The model fit to some of the spectra at 14 μm. The solid lines are observed spectra, and dash lines are for the C_2H_2 model and dash-dot line is for HCN. The excitation temperature of C_2H_2 is 500 K for all.

Figure 5. The comparison of band strength (height of Gaussian fit at 13.7 μm) for LMC stars (diamonds) and Galactic stars (filled circles). The Gaussian depth is relative to the continuum. There is no clear difference in line strength between Galactic and LMC samples. This band tends to become stronger towards redder stars, i.e. higher mass-loss rate stars. The crosses show the C_2H_2 model band strength at the excitation temperature of 500 K and the column density of 1×10^{17}, 3×10^{17}, and 1×10^{18} cm^{-2}. The horizontal scale of the crosses is arbitrary and is given such that the line connecting the crosses follows the observational tendency.

13.7 μm C_2H_2 band, which suggests that this band is formed throughout the circumstellar envelope.

To demonstrate that dilution by dust emission is not taking place, the 13.7 μm profile is fitted with a Gaussian, and the Gaussian height above the continuum is plotted as a function of colour (Fig. 5). The (pseudo-)continuum is estimated by linear interpolation of the spectra between 11.5–12.0 and 14.6–15.1 μm. The height from the Gaussian fit is divided by the value of the pseudo-continuum at the Gaussian centre. Using this ratio minimises the influence of the 14.0 μm HCN, which is important because HCN is often found among Galactic stars, but not in LMC stars. The continuum should also avoid the P- and R-branches of C_2H_2 as far as possible. We measured both the LMC spectra and the spectra of Galactic carbon stars reduced by Hony et al. (2002). The Galactic carbon stars are thought to be mostly located in the Galactic disk. Stars with strong HCN or 13.9 μm C_2H_2, such as W Ori, are not considered in this analysis, as the Gaussian fit failed. With the exception of IRAS 13416−6243, which is a post-AGB star exhibiting both PAH bands and the 13.7 μm C_2H_2 band, post-AGB stars and PNe are also excluded from this discussion.

Neither the Galactic nor LMC carbon stars show a decrease of the 13.7 μm C_2H_2 absorption band with redder infrared colour, i.e., with the optical depth of the dust shell. Moreover, the largest absolute values of Gaussian height tend to be found in stars with redder infrared colours among Galactic stars. The LMC stars show a smaller range in colour, but for the colour range of overlap there is little evidence for any difference between LMC and Galactic stars. All of the LMC stars show C_2H_2, but one Galactic star does not (IRC+20 326, Gaussian height of −0.03).

5 DISCUSSION

The shape of the 13.7 μm C_2H_2 feature is related to excitation temperature as demonstrated by Aoki et al. (1999) and Gautschy-Loidl et al. (2004). If the excitation temperature is about 1000 K, there is a broad wing longwards of 13.7 μm (seen in S Sct in Fig.3). Among our sample, there is no such a broad C_2H_2 band implying an excitation temperature much lower than 1000 K. Our observed spectra are reasonably well reproduced by C_2H_2 at 500 K (Fig. 2). This suggests that these molecular bands are of circumstellar, rather than photospheric, origin.

The fact that C_2H_2 becomes stronger rather than weaker towards redder stars suggests that 13.7 μm C_2H_2 originates outside of the region where warm dust is emitting, and is therefore much less subject to infilling by dust excess than are molecular bands from the photosphere.

Keady & Ridgway (1993) report that C_2H_2 can be detected throughout a shell, from the photosphere

up to the circumstellar envelope. Depending on the energy level, the dominant molecules for the line formation are located in different places in the photosphere or in the circumstellar envelope. The problem is that usually the inner hotter region shows a higher density and a higher temperature, and therefore a higher optical depth. Thus, the inner region will usually contribute more to the line formation.

The 13.7 μm C_2H_2 feature thus provides two self-consistent arguments for a molecular gas extended well into, and quite possibly beyond, the dust forming region. The gas is cool, and its features are not filled in by dust emission, because the 13.7 μm band arises from a cool layer of gas above the dust forming region.

The circumstellar C_2H_2 band strength does not show any particular metallicity dependence. Despite the lower metallicity in the LMC, the C_2H_2 Gaussian fit depths are comparable to those found in Galactic stars. Sloan et al. (2006) investigate carbon-rich stars in the Small Magellanic Cloud (SMC), whose metallicity is probably about a quarter of the solar value. They find that the C_2H_2 equivalent widths are higher among the SMC sample than among their Galactic counterparts. This may show the effect of carbon synthesised inside the AGB star and brought the surface by the third dredge-up. Newly synthesised carbon is more important for the C_2H_2 abundance than the effect of low initial metallicity and of low initial carbon abundance.

The increase of the 13.7 μm C_2H_2 depth with redder infrared colour (Fig. 5) indicates an increasing C_2H_2 column density. This is probably related to the mass in the circumstellar envelope. There are two possible reasons: the higher density may simply result in more C_2H_2 or the higher density may actually facilitate the formation of C_2H_2. There is a lot of scatter in a plot of 13.7 μm C_2H_2 against colour, suggesting that other effects such as abundance and temperature also influence the band strength. Alternative explanation for the scatter could include inner shocks caused by the pulsations (Gautschy-Loidl et al. 2004), as found in some variability in the colour and C_2H_2 index (Sloan et al. 2006).

There is no obvious detection of HCN among the LMC stars, apart from the suspected feature at 14.0 μm in MSX LMC 601 and TRM 88. While the absence of HCN features could result from HCN emission filling in an absorption feature, we consider this unlikely. Aoki et al. (1999) and Cernicharo et al. (1999) detected HCN emission in some Galactic carbon stars (only three stars out of the 9 stars they investigate), but one would expect to see other HCN bands at other wavelengths. Matsuura et al. (2005) and van Loon et al. (2006) report few detections of the HCN band at 3.5 μm in LMC stars compared to Galactic carbon stars. Furthermore, only two stars in the sample described here (NGC 978 IR4 and MSX LMC 494) show a suspected HCN band at 7 μm.

The lower HCN abundance is most likely explained as a result of lower abundance of nitrogen in a metal-poor environment. Nitrogen is produced but also destroyed in AGB stars and as a consequence will be much less abundant with respect to carbon in a metal-poor environment.

The HCN 14.0 μm strength at a column density of 3×10^{17} cm^{-2} is comparable to that of the 13.9 μm C_2H_2 band at a column density of 1×10^{18} cm^{-2} at 500 K (Fig. 2). If the low HCN abundance is responsible for the weak HCN features, the abundance of HCN could be less than one third of that of C_2H_2.

A chemical equilibrium model shows that the fraction of C_2H_2 in the atmosphere exceeds that of HCN at C/O$\sim$1.3, and it will be three times higher than that of HCN above C/O$>$1.7 (Matsuura et al. 2005). We assume that the oxygen and nitrogen abundances are [O/H] = 8.3, and [N/H] = 7.5. These elemental abundances are scaled from the solar elemental abundance (log[n(C)/n(H)]+12=8.56 and log[n(N)/n(H)]=8.05 (Anders & Grevesse 1989)) to the metallicity of the LMC, for which we adopt a value [Fe/H]=$-$0.6. The assumed oxygen and nitrogen abundances are comparable to those found in red giants in the LMC (Smith et al. 2002). The weak HCN but strong C_2H_2 bands may show that LMC carbon stars have a carbon abundance of [C/H] = 8.8–9.3.

A typical C_2H_2 column density of 1×10^{18} cm^{-2} can yield a mass-loss rate of $dM/dt = 3 \times 10^{-6} \times (r_{in}/R_*)$ M$_\odot$ yr^{-1}. The parameter r_{in}/R_* is the inner radius of the C_2H_2 line-forming region with respect to the stellar radius. We assume that the C_2H_2 abundance is 1×10^{-5} with respect to H$_2$ (Matsuura et al. 2005), that the expansion velocity is 20 km s^{-1}, and that the stellar radius R_* is 300 R$_\odot$. We also assume that the outer radius of the C_2H_2 circumstellar shell is much larger than the inner radius, and that the outer radius can be ignored for this calculation. If most of the C_2H_2 is formed at the photosphere (r_{in}/R_*=1), the mass-loss rate would be $dM/dt = 3 \times 10^{-6} M_\odot$ yr^{-1}. This would be the minimum gas mass-loss rate of our sample. However, the line-forming region is much further out, r_{in}/R_* would be larger than 1. 500 K corresponds to about 16 stellar radii or more (Höfner et al. 2003). This would be equivalent to a gas mass-loss rate of 5×10^{-5} M$_\odot$ yr^{-1} or higher.

van Loon et al. (2006) have estimated the mass-loss rate of 14 stars out of 26 in our sample by modelling the spectral energy distribution (SED). The mass-loss rate range from 9×10^{-6} M$_\odot$ yr^{-1} (NGC 1978-IR1) to 5×10^{-5} M$_\odot$ yr^{-1} (MSX LMC 635). Thus the two independent mass-loss rates, from our C_2H_2 and from the SED, are consistent. van Loon et al. (2006) use a gas-to-dust ratio of 500, based on the lower metallicity. These consistent mass-loss rates estimated from the C_2H_2 band and the SED may be supportive of such a high gas-to-dust ratio at low metallicity (van Loon et al. 2000).

6   CONCLUSION

We analyse molecular bands found in Spitzer spectra of LMC carbon stars. C_2H_2 bands are detected at 7.5 and 13.7 μm. The 13.7 μm C_2H_2 bands are of circumstellar origin. This is demonstrated by the absence of infilling

of this band by dust emission, even amongst stars with thick circumstellar envelopes, and because the excitation temperatures of C_2H_2 appear to be about 500 K. There are abundant C_2H_2 molecules despite the lower metallicity in the LMC compared to our Galaxy. This could be explained by carbon enrichment in the AGB stars. In contrast to C_2H_2 there is no clear evidence for HCN bands among the LMC sample, implying that low nitrogen abundances affect the HCN abundance.

We estimate from C_2H_2 gas mass-loss rates ranging from 3×10^{-6} $M_\odot$ yr^{-1} to 5×10^{-5} $M_\odot$ yr^{-1}. This is consistent with mass-loss rate estimated from the SED.

7   ACKNOWLEDGEMENTS

REFERENCES

Anders E., Grevesse N., 1989, Geochimica et Cosmochimica Acta 53, 197

Aoki W., Tsuji T., Ohnaka K., 1998, A&A 340, 222

Aoki W., Tsuji T., Ohnaka K., 1999, A&A 350, 945

Carter S., Mills I.M., Handy N.C. 1993, Journal of Chemical Physics, 99, 4379

Cernicharo J., Yamamura I., González-Alfonso E., de Jong T., Heras A., Escribano R., Ortigoso J., 1999, ApJ, 526, L41

Duari D., Hatchell J., 2000, A&A, 358, L25

Gautschy-Loidl R., Höfner S., Jørgensen U.G., Hron J., 2004, A&A 422, 289

Höfner S., Gautschy-Loidl R., Aringer B., Jørgensen U.G., 2003, A&A 399, 589

Hony S., Waters L.B.F.M., Tielens A.G.G.M., 2002, A&A 390, 533

Houck J.R., Roellig T.L., van Cleve J., et al., 2004, ApJS 154, 18

Hron J., Loidl R., Höfner S., Jørgensen U.G., Aringer B., Kerschbaum F., 1998, A&A 335, L69

Jacquemart D., Mandin J.-Y., Dana V., et al., 2003, Journal of Quantitative Spectroscopy & Radiative Transfer 82, 363

Keady J.J., Hinkle K.H. 1988, ApJ 331, 539

Keady J.J., Ridgway S.T., 1993, ApJ 406, 199

Kraemer K.E., Sloan G.C., Price S.D., Walker H.J., 2002, ApJS 140, 389

Matsuura M., Yamamura I., Cami J., Onaka T., & Murakami H., 2002a, A&A 383, 972

Matsuura M., Zijlstra A.A., van Loon J.Th., et al., 2002b, ApJ 580, L133

Matsuura M., Zijlstra A.A., van Loon J.Th., et al., 2005, A&A 434, 691

Millar T.J., Herbst E., Bettens R.P.A., 2000, MNRAS 316, 195

Rothman L.S., Jacquemart D., Barbe A., et al., 2005, Journal of Quantitative Spectroscopy & Radiative Transfer 96, 139

Sloan G.C., Kraemer K.E., Matsuura M., Wood P.R., Price S.D., Egan M.P., 2006, ApJ 645, in press

Smith V.V., Hinkle K.H.. Cunha K. et al., 2002, AJ 124, 3241

Smith V.V., Lambert D.L., 1985, ApJ 294, 326

Tsuji T., 1981, JApA 2, 253

van Loon J.Th., 2000, A&A 354, 125

van Loon J.Th., Zijlstra A.A., Groenewegen M.A.T., 1999, A&A 346, 805

van Loon J.Th., Marshall J.R., Cohen M., Matsuura M., Wood P.R., Yamamura I., Zijlstra A.A., 2006, A&A 447, 971

Zijlstra A.A., Matsuura M., van Loon J.Th., et al., 2006, MNRAS, accepted